THE RATE AND THE MECHANISM OF THE REACTIONS OF HYDROGEN SULFIDE WITH THE BASIC MINERALS IN COAL

A. Attar and F. Dupuis

Department of Chemical Engineering

University of Houston

1.0 INTRODUCTION

The inorganic matter in coal can be classified into three groups of minerals according to their reactions with hydrogen sulfide (H_2S): (1) basic minerals, (2) minerals with catalytic activity, and (3) inert minerals. In the range of temperatures 200-900°C, most of the minerals are inert or have a slight catalytic activity on the rate of decomposition of H_2S. However, the basic minerals react with H_2S and the corresponding sulfides are formed. The most important minerals in this category are calcite (trigonal $CaCO_3$), aragonite (orthorhombic $CaCO_3$), dolomite ($CaCO_3 \cdot MgCO_3$), sidrite ($FeCO_3$), and to some extent montmorilonite (clay) (Attar, 1977).

The systems of reaction between H_2S and a metal carbonate MCO_3 involves four reactions (Glund et al., (1930), Stinnes (1930), Bertrand (1937), Parks (1961), and Squires (1972)).

1. Direct reaction of the carbonate with H_2S:

$$MCO_3 + H_2S \rightarrow MS + H_2O + CO_2 \qquad (1)$$

2. Decomposition of the carbonate to the oxide MO and CO_2:

$$MCO_3 \rightarrow MO + CO_2 \qquad (2)$$

3. Reaction between the oxide and H_2S:

$$MO + H_2S \rightarrow MS + H_2O \qquad (3)$$

4. Sintering of the oxide and the formation of non-porous materials.

$$\text{porous MO} \xrightarrow{\Delta} \text{non-porous MO} \qquad (4)$$

Reactions 1. and 2. are parallel, and reactions 3. and 4. are parallel. The last two reactions are in series with reaction 2.

$$\begin{array}{lll} & & \xrightarrow{\Delta} \text{non-porous MO} \\ & \xrightarrow{\Delta} CO_2 + MO & \xrightarrow{H_2S} MS + H_2O \\ MCO_3 & & \\ & \xrightarrow{H_2S} MS + CO_2 + H_2O & \end{array} \qquad (5)$$

H_2S is formed in coal by the reactions of FeS_2 with hydrocarbons and H_2, (Powell, 1921) and by the decomposition of the organic sulfur compounds Thiessen (1945). In particular, H_2S is formed when the sulfidic functional groups decompose to H_2S and an olefin. The H_2S can react with the basic minerals and thus, the sulfur is trapped in the char in the form of the sulfide (Armstrong 1939). The kinetics of the reactions of H_2S with calcined dolomite and calcite were studied by Squires and co-workers (1970, 1972). In the present work, the mechanism of the reaction, their rate, and rate constants were derived for the reactions of H_2S with calcite, sidrite, dolomite, and montmorilonite.

Complete conversion of dolomite to CaS and $MgCO_3$ is obtainable at 570°C, but only 1.8-2.9 Wt. % of -200 mesh calcite reaction at these conditions (2.1 m^2/gm surface area). At 700°C calcite and dolomite react at essentially identical rates. The rate of reaction of dolomite is however very sensitive to impurities.

Different rate controlling steps limit the apparent rate of consumption of H_2S at different temperatures. The rate controlling step depends also on the particular material and on its crystalline structure. At low temperatures, the rate is controlled by the rate of mass transfer and by the rate of diffusion of CO_2 in MS. At intermediate temperatures, the rate of consumption of H_2S is controlled by the availability of free surface of MO or MCO_3. In this range of temperature, the carbonates decompose according to reaction 2, a new surface is thus exposed which is not covered by MS, thus, the effective rate of consumption of H_2S increases. The available surface decreases by sintering when the temperature is too high, thus the rate of consumption of H_2S may decrease. When the rate of decomposition of MCO_3 becomes very large, the rate of consumption of H_2S may be limited by mass transfer in the gas.

The crystalline structure of calcite and dolomite is trigonal (Bragg et al. (1965) p. 127) and is basically identical, except that in dolomite alternate Ca^{+2} ions are replaced by Mg^{+2} ions. The spacial dimensions are different because the ionic radius of Mg^{+2} is 0.65 A and that of Ca^{+2} is 0.99 A (Greenwood, 1970). The mechanism of their reaction is however very different.

The rate of reaction of pure dolomite with H_2S is almost constant, and, does not vary with the conversion (up to 30 Wt. % conversion). Impure dolomite reacts initially at a much larger rate then after some of it had been converted. At 570°C the rate drops to about half the initial rate after about 4% of the material had been converted. At 570°C calcite reacts initially at about the same rate as pure dolomite, however, the rate of reaction drops to nil very rapidly. We estimate that when a layer of about 7.8 molecules of CaS, on the average, is formed on the surface of calcite, the diffusion of H_2S is blocked and the reaction stops. The layer of CaS breaks at around 635-650°C when the "pressure" of CO_2 inside the $CaCO_3$ crystal due to the decomposition reaction

$$CaCO_3 \rightarrow CaO + CO_2 \qquad (7)$$

becomes excessive. When the CaS layer breaks, a new surface is exposed and the reaction can proceed. Around 700°C no difference could have been detected between the rate of reaction of calcite and dolomite.

2.0 EXPERIMENTAL

Figure 1 is a schematic flow diagram which shows the relations among the various parts of the system.

The experimental system consists of four major components: (1) a differential reactor, (2) a pulse injector, (3) a gas chromatograph with a TC detector, and (4) an integrator with a data system.

Figure 2 shows the differential reactor. The shell (1), the tube (2), and the fillers (3) are made out of quartz. The gas inlet and outlet are through a SS connector. The quartz reactor is inserted through the wall of a high temperature furnace which temperature is controlled and monitored.

Pulses of the reactive gas, H_2S, are fed using a microprocessor controlled gas-chromatograph injector. The size of the injector loop determines the size of the pulse of H_2S which is introduced into the stream of helium. The helium passed through the reactor and into a chromatographic column and detector.

Each pulse of H_2S which is injected into the reactor resulted in a pulse which consists of the reaction products plus the unreacted H_2S. The mixture of gases is separated on the column and detected by the TC detector. The signal from the detector is integrated by a microprocessor which multiplies the areas by the proper calibration factors and prints the amounts of each component in the pulse of products of the reaction. The integrator and the injector are synchronized so that periodic operation is possible.

The repeatability of the injections was 0.05% or better. The overall accuracy of the analysis was at least 10% and usually better than 2% based on material balance.

Mixtures of H_2S, CO_2, and H_2O were separated on a 6' X 1/8" column of chromosorb 103 80/100 mesh at 90°C. The helium flow was 75 ml/min.

The various minerals that were tested were NBS standard minerals,* except for the calcite which was purchased from Fisher Scientific.

*We wish to thank Dr. J. C. Butler, chairperson of the Department of Geology, University of Houston, who gave us the minerals.

3.0 MATHEMATICAL ANALYSIS

The rate of the reaction $\bar{r}$ can be estimated using the relation:

$$\bar{r}_i = \frac{q(W_o - W_i)}{W_s W_o} = \alpha \frac{qPi}{W_s W_o} \tag{8}$$

where q is the carrier rate of flow, W_s the weight of material in the reactor, W_o the number of moles that were injected in a pulse, W_i the number of moles of unreacted products, Pi the number of moles of products, and α a stoichiometric coefficient.

The rate of consumption of the solid in the reactor depends on the amount of solid, A, and on the instantaneous concentration of gas, C, around it; several cases deserve special attention and will be discussed in detail. Extention of the theory to other cases is straight forward.

3.1 Rate of Reaction Depends on n-Power of the Solid

When the rate of reaction depends on the n-th power of the weight of the solid in the reactor, A, then:*

$$-\frac{dA}{dt} = kA^n C \tag{9}$$

It is assumed for the moment that only one reaction takes place. If we multiply equation (9) by q, the volumetric rate of flow of the gas, and rearrange the equation we obtain:

$$-\frac{q}{1-n}\, d(A^{1-n}) = kqc \cdot dt \tag{10}$$

Integration of the equation for the i-th pulse yields

$$-\frac{q}{1-n}\,(A_i^{1-n} - A_{i-1}^{1-n}) = \int_{t_i}^{\infty} kqc_i dt \tag{11}$$

If the reaction is isothermal and only a small fraction of the pulse is consumed, thus the lower bound on k, k_1, can be obtained by taking c = c (feed)

$$\int_{t_i}^{\infty} k_1 qcdt = k_1 \int_{t_i}^{\infty} qc_i dt = k_1 W_i \tag{12}$$

where W_i is the number of moles of H_2S that were injected in the i-th pulse. Combining the last two equations yields:

$$\frac{A_i}{A_{i-1}} = \left[1 - \frac{(1-n)k_1 W_i}{q\, A_{i-1}^{1-n}}\right]^{\frac{1}{1-n}} \tag{13}$$

*This assumption is equivalent to saying that the rate of the reaction depends on a property of the solid which depends on the n-the power of its weight e.g., the surface area is roughly proportional to $A^{2/3}$.

If $A_i \approx A_{i-1} \approx A_o$ and $W_i = W$ = constant for all i-s then

$$\frac{A_i}{A_o} \cong \left[1 - \frac{B}{A_o^{1-n}}\right]^{\frac{i}{1-n}} \tag{14}$$

where $B = \dfrac{(1-n)k_1 W}{q}$ (15)

Equation 14 can be used to evaluate B from which the rate constant k can be determined.

When a small fraction of the material is converted, $A_i \approx A_o$, a plot of $\log \frac{A_i}{A_o}$ vs. i yields a straight line with the slope $\frac{1}{1-n} \log (1 - \frac{B}{A_o^{1-n}})$. To evaluate n, several experiments should be carried out with different initial amounts of the solid A_o, or with pulses with a different size, W.

The upper bound on the rate constant k, k_u, can be estimated using the value of c at the outlet:

$$C = \frac{qC_o}{q + \alpha k A^n} \tag{16}$$

where Co denotes the concentration of the gas in the feed; and α is a coefficient to account for differences in the stoichiometry. Substitution of equation (16) in equation (9) yields:

$$\frac{q}{k_u(1-n)} (A_i^{1-n} - A_{i-1}^{1-n}) + \alpha (A_i - A_{i-1}) = -W_i \tag{18}$$

From stoichiometry:

$$\alpha (A_{i-1} - A_i) = (W_i - W_{iout}) \tag{19}$$

Therefore:

$$\frac{q}{k_u(1-n)} (A_i^{1-n} - A_{i-1}^{1-n}) = -W_{iout} \tag{20}$$

or

$$\frac{A_i}{A_{i-1}} = \left[1 - \frac{k_u(1-n)W_{iout}}{q\, A_{i-1}^{1-n}}\right]^{\frac{1}{1-n}} \tag{21}$$

A very important special case is when $n = \frac{2}{3}$. This occurs when the rate of reaction depends on the available surface area. When the solid is "infinitely porous" it may be 1. The case where $n \neq 1$ in the following section.

3.2 Rate of Reaction Proportional to the Weight of the Solid

If all the amount of the solid in the reactor is equally available for reaction, the rate may depend on the first power of the weight of the solid.

$$-\frac{dA}{dt} = kAC \tag{22}$$

The lower bound on the rate constant can be evaluated from the equation:

$$\ln \frac{A_i}{A_{i-1}} = -\frac{k_l}{q} W_i \tag{23}$$

Equation (23) can be simplified if the size of the pulses is equal, namely $W_i = W$ for all i. Then:

$$\frac{A_i}{A_o} = e^{-\frac{k_e W}{q} i} = e^{-\gamma i} \tag{24}$$

$$\gamma = \frac{k_e W}{q} \tag{25}$$

A plot of $\log \frac{A_i}{A_o}$ vs. i should yield a straight line with the slope γ, when such a model holds.

The upper bound on k, k_u, can be evaluated using the equation:

$$\frac{A_i}{A_{i-1}} = e^{-\frac{k_u W_i}{q}} \tag{26}$$

or

$$\frac{A_i}{A_o} = e^{-\frac{k_u}{q} \sum_o^i W_i} \tag{27}$$

3.3 Evaluation of the Rate Constants from Experimental Data

The data that are derived in each experiment include the initial condition of the sample, its weight, W_s, and its specific surface area, s_a. The length of the cycle, θ_c is usually determined by the difficulty of the separation of the products. The number of moles of reactive gas per injection, W, is determined by the fineness of the resolution which is required or by the sensitivity of the experimental system. The value of q can be used to modify B or γ, however it is usually dictated by the separation procedure.

The area of the pulse of gas when no reaction occurs is denoted by S_o. The area of the peak of unreacted gas from the i-th pulse is denoted by S_i, and the area of the peak of the i-th product from the i-th pulse is denoted by K_j, where the response to the pulsed gas is taken as a unity. The total weight of solid in the reactor can react with the stoichiometric

amount of gas, W_g; the equivalent area that a peak of magnitude W_g would have had it denoted by S_T. It is assumed that the detectors are linear, therefore, when all the weight of the solid is available for the reaction:

$$\phi_i = \frac{A_i}{A_o} = 1 - i\frac{S_o}{S_T} + \frac{\Sigma S_i}{S_T} \tag{28}$$

The average rate of consumption of gas per unit mass of solid is:

$$\bar{r}_i = \frac{q(S_o - S_i)}{W_s\ S_o} \tag{29}$$

The rate of the single reaction which produces the j-th product is:

$$\bar{r}_i = \alpha\frac{q\ S_{ji}}{K_j S_o W_s} \tag{30}$$

Note that if only part of solid, e.g. only a surface layer on the top of each crystal reacts, then S_T will have to be determined experimentally from the relation:

$$S_T = \sum_{i=1}^{\infty} (S_o - S_i) \tag{31}$$

4.0 RESULTS

The most important variables that affect the rate of the consumption of H_2S are the temperature, the time-temperature history of the sample, the initial conditions of the sample, and the conversion.

Two types of kinetic experiments were conducted: (1) "isothermal," and (2) "temperature programmed." In each experiment, pulses of H_2S with a fixed size were injected, and the amounts of CO_2, H_2O and unreacted H_2S were determined. In addition, the raw carbonates were tested by DTA and their specific surface area was determined by N_2 adsorption.

Arguments of material balance can be used to deduce the following conclusions: (1) The total number of moles of MS that are formed is equal to the total number of moles of H_2S that are consumed; and also to the number of moles of water that are produced. (2) The number of moles of H_2O and of CO_2 that are produced in reaction 1 as a result of a given pulse of H_2S, is equal to the number of moles of H_2S that are consumed in the reaction. The number of moles of H_2O, in excess to the number of moles of CO_2, are formed by reaction 3. Figure 3 shows the isothermal rate of consumption of H_2S by calcite, pure dolomite, dolomite, montmorilonite, and sidrite at 570°C, as a function of the conversion of the solid. The rate of the reaction with H_2S behaves according to one of three modes: (1) rate independent of the conversion, (2) rate decreasing with the conversion, but complete conversion is obtainable, (3) rate decreasing very rapidly with the conversion, and complete conversion is not obtainable.

The rate of reaction of dolomite at 570°C as a function of the conversion is almost constant. However, at 700°C the rate decreases slowly with the conversion. The rate of reaction of calcite at 570°C decreases very sharply, and becomes essentially zero after about 2.8% of the material are converted. At 700°C the rates of conversion of dolomite and calcite to MS are the same.

Sidrite decomposes at much lower temperatures than $CaCO_3$ or dolomite, FeO and CO_2 are formed. The decomposition of sidrite is complete at 495°C, FeO sinters much more rapidly then CaO. Thus the available surface area of FeO decreases when the sidrite is heated for prolonged times above 500°C. Figure 4 shows the rate of consumption of H_2S by decomposed sidrite that was kept 2-1/4 and 5-1/4 hours at 635°C.

Figure 5 shows the rate of consumption of H_2S by calcite, dolomite, and sidrite which temperature was increased at about 3.3 °C/min. The data were not corrected for the conversion of the material; the effect of the correction is more important at the higher temperatures. The rate of consumption of H_2S by calcite and dolomite seems to be very similar above 650°C, however, different rates are observed below 650°C. Figure 6 shows the rate of evolution of CO_2 from calcite and dolomite as a result of reaction 1. The data show very clearly that the rate of evolution of CO_2 from calcite decreases with the temperature up to 635°C but then it increases very rapidly and at about 700°C it becomes identical to the rate of evolution of CO_2 from dolomite. The rate of evolution of CO_2 from dolomite increases monotonically with the temperature. It should however be noted that the apparent decrease in the rate is due to the coverage of the surface by CaS and the creation of resistance to mass transfer of CO_2. (The plotted rate is not the initial rate of reaction of clean surfaces). The rate of evolution of CO_2 that results from the thermal decomposition of the carbonate, shows as a continuous drift in the detector base line. The decomposition of calcite and dolomite to CaO were complete at 810°C and the decomposition of sidrite was complete at 495°C. Figure 7 shows the rate of formation of water by reaction 3. The data show that the rate of evolution of water becomes almost constant at temperatures above 685°C where no more CO_2 is formed by reaction 1.

5.0 DISCUSSION OF THE RESULTS

The discussion is divided into two parts: discussion of the mechanism of the reactions, and discussion of the rates of the reactions.

5.1 The Mechanism of the Reactions

The rate of consumption of H_2S is influenced by the rates of reactions 1-4, which takes place simultaneously, and by the rate of mass transfer of H_2S, H_2O, and CO_2 through the layer of product MS which is formed on the surface of the MCO_3 crystals. The rate of the chemical reactions is a a strong function of the temperature, therefore, different reactions may dominate at different temperatures. In particular, the rate of decomposition of $CaCO_3$ and of dolomite (reaction 2) becomes very large at temperatures above 739°C. Therefore, large amounts of MO are produced

which competes with the MCO_3 on the available H_2S. Since CaO reacts with H_2S more rapidly than $CaCO_3$, the apparent rate of consumption of H_2S by the mixture of CaO-$CaCO_3$ at temperatures above 730°C is significantly larger then at lower temperatures. Mass transfer in the gas may also become the limiting step at very high temperatures.

The rate of mass transfer in the solid may limit the apparent rate of reaction by preventing the reagent H_2S from reaching the reaction metered, or by preventing the products CO_2 and H_2O from escaping out. The role that the product MS plays depends on the crystalline structure of MS and that of "host" crystal, the MO or the MCO_3. If the crystalline structures of MS and the host are "compatible" so that the layer of MS can adhere to the surface of the host, (as a solid solution) then resistance to mass transport will be created as a result of the reaction.

Figure 3 shows that at 570°C calcite stops to react after about 2.8 Wt. % of the -200 mesh material was converted. Dolomite, which has the same crystalline configuration continues to react although the initial rate of the reaction depends on the impurities in the material. Dolomite and calcite have the same crystalline structure, except that in dolomite every alternate Ca^{+2} ion is replaced by a Mg^{+2} ion. Had all the components of dolomite been reactive, one would expect that MgS and CaS will be formed as a result of the reactions with H_2S. However, at 570°C only CaS is formed since $MgCO_3$ does not react with H_2S at 570°C. Therefore, a continuous layer of CaS can not be formed on the surface of dolomite but it can be formed on the surface of calcite. Therefore, once a layer of average thickness of about 7.8 molecules is formed on the surface of the calcite, at least one of the gases CO_2, H_2O, or CO_2 can not diffuse through it anymore and reaction 1 stops.

It is plausible that the reaction between H_2S and calcite stops because CO_2 cannot diffuse through a layer of CaS. One evidence which supports this theory is that CaO reacts with H_2S according to reaction 3 and is completely converted to CaS. Had CaS been impermeable to H_2O or to H_2S, the reaction of CaO should have also stopped before complete conversion to CaS.

The latter theory is supported by the experimental evidence of CO_2 by retention 1 and of the absorption of H_2S by reactions 1 and 3 as a function of the temperature. The experiment was conducted as follows: first the surface of the calcite was reacted with H_2S at 590°C until the reaction stopped, and then the temperature was programmed up slowly while injecting small pulses of H_2S to study the reactivity of the material. The data shows clearly that around 640°C the layer of CaS breaks, new surfaces of CaO + $CaCO_3$ are exposed and reactions 1 and 3 can commence. The equilibrium pressure of CO_2 at 640°C is estimated to be about 0.02 atms. Such a pressure is apparently sufficiently large and can break the layer of CaS.

The crystalline structures of FeO and FeS are different and apparently FeS does not adhere to the surface of FeO. Indeed, even if it adheres,

FeS seems to permit diffusion of H_2S since reaction 3 can proceed at 570°C into completion. However, limited resistance to mass transfer is observed when 3-4 Wt. % of the material is converted.

FeO sinters at a much larger rate than CaO, and at high temperatures its available surface area decreases very rapidly with time. Figure 8 shows that at 570°C, equation (14) with n = 2/3 fits the data very adequately, but at 635°C or 700°C the description is inadequate. Equation (14) was derived from equation (9) in which the sintering effect which reduces the surface area was not taken into consideration. Note that an increase in the temperature results in an increase in the rate constant of reactions 3 and 4. The latter reaction reduces the surface area which is available for reaction with H_2S according to reactions 1 and 3.

5.2 Quantitative Rate Data

Rate data on some selected systems is presented in Table 2. The data were derived on samples of particles -200 mesh, of about 0.1-0.2 gm each. Unless otherwise specified, the material was permitted to equilibriate 2-1/4 hours at the reaction temperature. Equation (14) with n = 2/3 has been used to evaluate the lower bound on the rate constant.

The evaluation of the activation energies and their use should be done with caution, since they have greatly different values in different temperature regions. A summary of the data is given in Table 2.

TABLE 2

Activation Energies for the Rate of Consumption of H_2S by Minerals

Material	T°C Range	Controlling Mechanism	Ea kcal/mole ±30%
Calcite	560	Diffusion of gas through CaS	0.0
Calcite (with CaO)	560-670	Rate of reaction	19.0
Calcite (with CaO)	670	Rate of gas-phase mass transfer	4.0
Dolomite	640	Rate of reaction	12.2-13.5
Dolomite (with $CaO \cdot MgCO_3$)	640	Rate of gas-phase mass transfer	2.4
Sidrite (with FeO)	460	Rate of reaction	15.2
FeO	460	Rate of gas-phase + mass transfer and sintering	0.0

In general, mass transfer controls when the reacting material is a carbonate, and the rate of reaction (2) or the rate of gas-phase mass transfer will control when the reacting solid is the oxide. Small activation energies (0-4 kcal/mole) are observed when the carbonate reacts and 30-45 kcal/mole are observed when the oxide reacts. Note should however be made of the decomposition reaction 2 in which the carbonate is transformed into an oxide. This reaction can not be controlled and it tends to activate the solid even when the carrier gas contains CO_2 (the rate of reaction 2 is suppressed in the latter case).

REFERENCES

Armstrong, V. and Himms, G. W., Chem. and Ind., June 10, 543 (1939).

Attar, A., "The Fundamental Chemistry and Modeling of the Reactions of Sulfur in Coal Pyrolysis," Paper presented in the AIChE Meeting, Houston, Texas, March 1977.

Attar, A., "The Fundamental Chemistry and Modeling of the Reactions of Sulfur in Coal Pyrolysis and Hydrogenation," In print in a Chemical Engineering Progress technical manual.

Bertrand, M. F., "Gas Purifying Materials," Brit. Pat., 462, 934 (1937). C.A. 31-6446.

Bragg, L. and Claringbull, G. F., "Crystal Structures of Minerals," Cornell University Press, Ithaca, N. Y. (1965).

Gluud, W., Keller, K., Klempt, W., and Bertehorn, R., "Development and Operation of a New Process for Hydrogen and Hydrogen-Nitrogen Mixtures," Ber. Ges. Kohlentech., 3, 211 (1930).

Greenwood, N. N., "Ionic Crystals, Lattice Defects and Nonstoichiometry," Butterworths, London (1970).

Parks, G. D., "Mellons Modern Inorganic Chemistry," Longvans, London (1961).

Powell, A. R., Ind. Eng. Chem., 13, 33 (1921).

Ruth, L. A., Squires, A. M., and Groft, R. A., "Desulfurization of Fuels with Calcined Dolomite," Paper presented in the ACS Meeting, Los Angeles, California, March (1971).

Squires, A. M., "New Systems for Clean Power," Int. J. Sulfur Chem., Part B, 7 (1), 85 (1972).

Stinnes, G. M., "Gas Purifying Materials," Brit. Pat., 371, 117 (1930). C.A. 27-2565.

Thiessen, G., "Forms of Sulfur in Coal," Chapt. 12, p. 475 in "Chemistry of Coal Utilization," Lowry, H. H., (ed.), Wiley, N. Y. (1945).

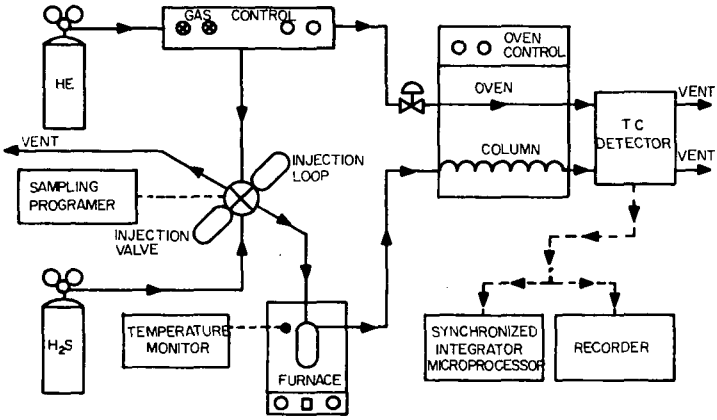

FIGURE 1: SCHEMATIC DIAGRAM OF EXPERIMENTAL SYSTEM

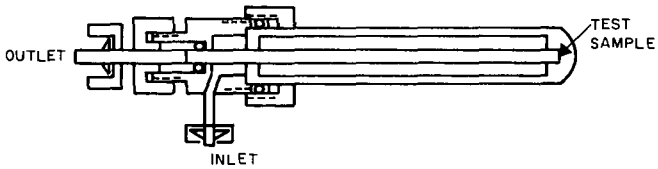

FIGURE 2: CROSS SECTION OF THE HIGH TEMPERATURES MICRO-DIFFERENTIAL REACTOR.

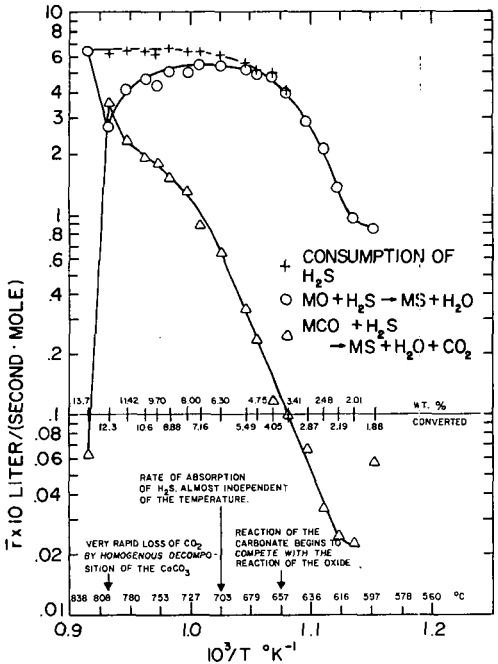

FIGURE 7 : RATE OF CONSUMPTION OF H_2S AND THE RATES OF EVOLUTION OF H_2O AND CO_2. THE TEMPERATURE WAS PROGRAMMED UP AFTER THE REACTION AT 590°C STOPPED. SEE TEXT.

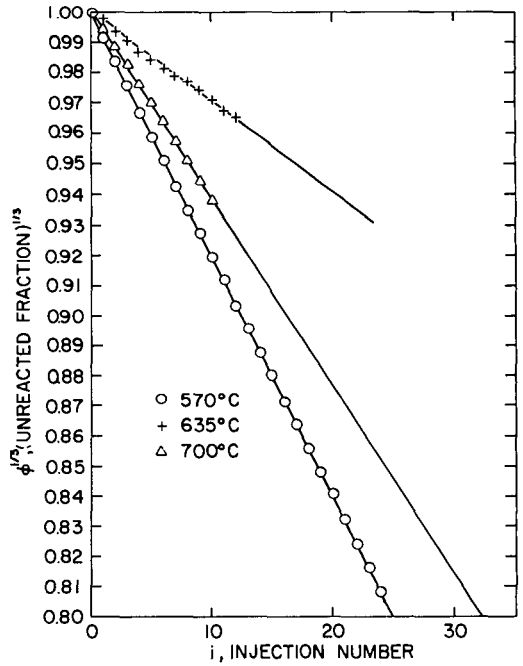

FIGURE 8 : THE PROGRESS OF THE REACTION OF SIDRITE AT DIFFERENT TEMPERATURES.

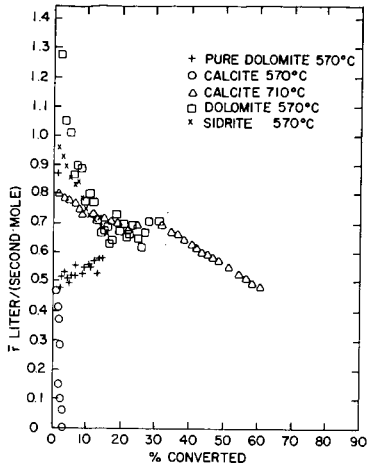

FIGURE 3: THE RATE OF CONSUMPTION OF H_2S BY BASIC MINERALS.

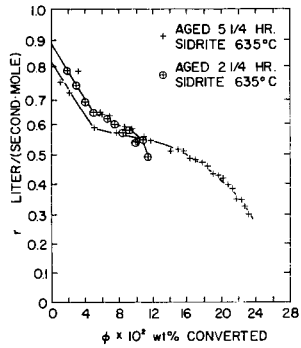

FIGURE 4: THE RATE OF CONSUMPTION OF H_2S BY DECOMPOSED -200 MESH SIDRITE AT 635°C

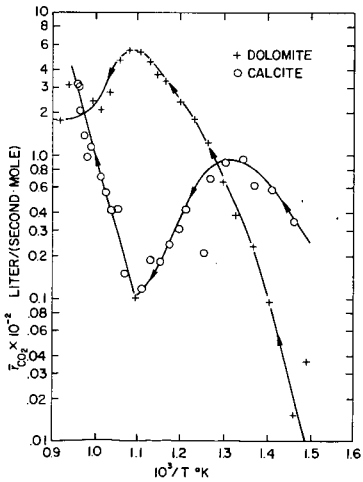

FIGURE 6: RATE OF EVOLUTION OF CO_2 FROM CALCITE AND DOLOMITE IN A TEMPERATURE-PROGRAMMED TEST.

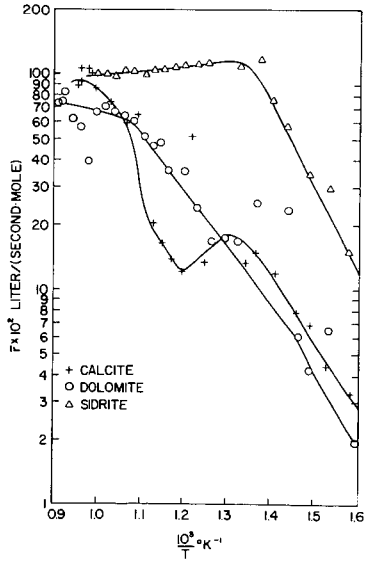

FIGURE 5 THE VARIATION IN THE RATE OF CONSUMPTION AT H_2S BY BASIC MINERALS IN TEMPERATURE PROGRAMMED EXPERIMENTS.